Supramolecular Chemistry
Publication details, including instructions for authors and subscription information:
http://www.informaworld.com/smpp/title~content=t713649759

Ordered Peptide Assemblies at Interfaces

Hanna Rapaport[a]
[a] The Department of Biotechnology Engineering, Ben-Gurion University of the Negev, Beer-Sheva, Israel

To cite this Article Rapaport, Hanna(2006) 'Ordered Peptide Assemblies at Interfaces', Supramolecular Chemistry, 18: 5, 445 — 454
To link to this Article: DOI: 10.1080/10610270600665905
URL: http://dx.doi.org/10.1080/10610270600665905

Supramolecular Chemistry, July–August 2006 Vol. 18 (5), pp. 445–454

Taylor & Francis
Taylor & Francis Group

Ordered Peptide Assemblies at Interfaces

HANNA RAPAPORT*

The Department of Biotechnology Engineering, Ben-Gurion University of the Negev, Beer-Sheva, 84105 Israel

(Received 30 December 2005; Accepted 1 March 2006)

Molecular systems composed of peptides or proteins can be programmed to yield intriguing and potentially useful supra-molecular architectures. In the past decade peptide self-assemblies at interfaces have been the subject of various studies aiming at formation of molecular structures with predictable patterns and properties. Most of these systems utilized amphiphilic peptides, usually of a particular secondary structure, that self-assemble through non-covalent intermolecular interactions, into two-dimensional, organized supramolecular structures. The interest in design and preparation of self-assembled functional materials is driven by potential benefits to nanotechnology and nanobiotechnology. This review is restricted to amphiphilic peptide assemblies at interfaces studied by grazing incidence X-ray diffraction and atomic force microscopy, geared towards nanometer-scale structural characterizations.

Keywords: amphiphilic beta-sheet; alfa-helix; Langmuir Blodgett; AFM; GIXD

INTRODUCTION

The evolving field of molecular self-assembly aims at designing the shape of multi-molecular clusters by controlling intermolecular interactions [1,2]. In the search for advanced materials amenable to self-assembly there has been growing interest in the intriguing peptide and protein architectures. In particular, amphiphilic peptides, which display hydrophobic and hydrophilic amino acids may induce particular folds that are sequence dependent. Since the fifties of the past century amphiphilic polypeptides have been attracting interest as a class of polymers and as protein analogs [3–5]. Back then, these systems have been studies at interfaces, mostly by Langmuir techniques, spectroscopic measurements [6–8] and upon appropriate sample preparations also by electron or X-ray diffraction [3]. Nevertheless, these techniques could not provide direct information on the molecular order at interfaces or the extent of order at the nanometer length scale.

Current studies of peptide assemblies at interfaces take advantage of various surface sensitive analytical tools, a few of which provide in-situ sub-molecular structural description. One approach involves the use of grazing incidence X-ray diffraction (GIXD) from synchrotron source for probing ordered molecular assemblies within Langmuir films at the air–water interface [9]. The compounds commonly studied by GIXD constitute long chain hydrophobic tails with a hydrophilic head group. The relatively high stability and uniformity of these systems at air–water interface yields high quality diffraction patterns that may be attributed detailed molecular structure models. Progress in the design and characterization of ordered Langmuir films at interfaces [9] also by atomic force microscopy (AFM), provides strong incentives to apply similar methodologies to the study of the relation between amino acid sequence, secondary structure formation and intermolecular interactions leading to peptide self-assembly at interfaces.

Many of the peptide examined at interfaces utilize secondary structural elements of proteins, i.e. β-strands, helices and turns in engineered molecular arrangements, amenable to the design of functional nanostructures [10,11]. Ordered amphiphilic peptide monolayers at interfaces may provide planar scaffolds relevant to a broad spectrum of potential applications in nanometer-scale surface patterning. By combining self-assembled molecular systems with current lithography techniques [12] sophisticated molecular architectures may be developed. Ordered peptide assemblies at interfaces may

*Corresponding author. E-mail: hannarap@bgumail.bgu.ac.il

ISSN 1061-0278 print/ISSN 1029-0478 online © 2006 Taylor & Francis
DOI: 10.1080/10610270600665905

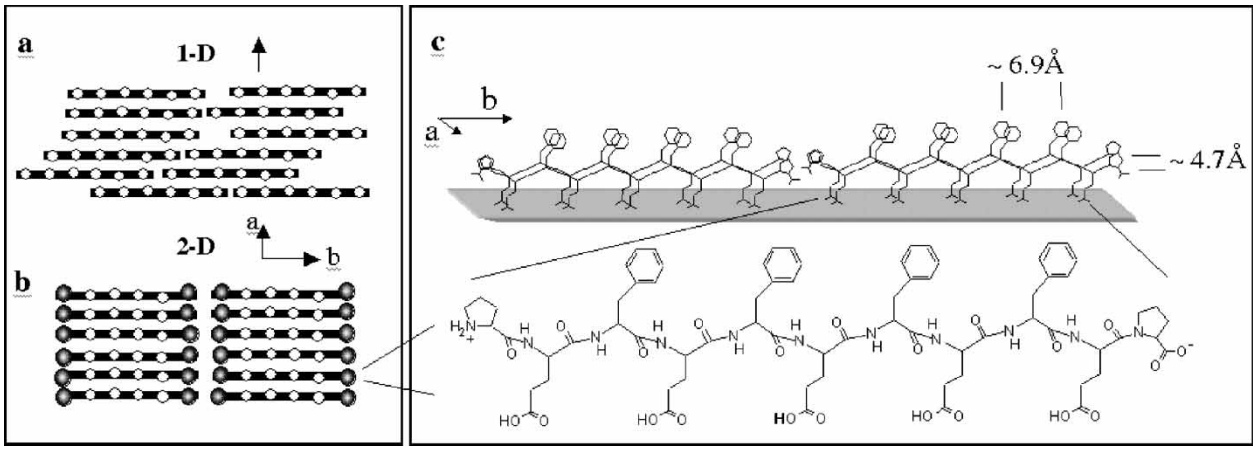

FIGURE 1 Schematic diagrams of β-strand assemblies at the air water–interface, (rods and open dots represent peptide backbones and hydrophobic amino acids respectively). View down the normal to the β-sheet of (a) one-dimensional order and (b) two-dimensional order induced by distinct chain termini (filled dots). (c) Schematic representation of the peptide Pro–Glu–$(Phe–Glu)_4$–Pro in the β-pleated conformation and the targeted β-sheet crystalline assembly at the air–water interface. An estimate of the area per molecule can be obtained using the repeat distances of ~4.7 and ~6.9 Å that have been observed previously in crystalline β-sheet structures (e. g. $4.7 \times 6.9 \times 5.5 = 178\,Å^2$ for the 11 residue peptide). Reprinted with permission from ref. [17]. (Copyright 2000 American Chemical Society.)

provide planar nanometer-scale molecular scaffolds, relevant to photoreactive films [13], molecular electronic devices [14], cell guidance substrates [12], long-range alignment of nanocrystals [15], biomineralization [16] and more. Systematic design strategies, coupled with structural characterization and molecular modeling would enable the realization of nanometer scale applications.

This review is restricted to structural studies of amphiphilic peptides monolayers at interfaces that rely mainly on GIXD of Langmuir films at air–water interface and on AFM studies geared towards nanometer scale resolution structural characterizations. The amphiphilic peptide systems that have so far been examined by GIXD may be divided into two main categories, i.e. β-sheets and helices.

SINGLE STRANDED ANTIPARALLEL β-SHEETS

Peptides comprising repetitive dyads of hydrophilic and hydrophobic amino acid residues tend to adopt β-pleated sheet arrangements in particular at hydrophilic–hydrophobic interfaces. Local order within monolayers of such peptides at the air–water interface may be inferred from infrared and circular dichroism measurements [8]. Spectroscopic data do not, however, provide information on extended order, *i.e.*, molecular order on the nanometer length scale. Moreover, the flexibility of the peptide backbone and, the repetitive nature of the amino acid sequence may induce nematic-like assembly (Fig. 1a) that exhibits mostly one-dimensional order (1-D), in the direction normal to the peptide backbone. Molecular assemblies with predominantly 1-D order will exhibit absorption spectra typical of β-sheet structures that are not necessarily organized in two-dimensional (2-D) assemblies. The typical distance between every second amino acid in a b-pleated peptide is ~6.9 Å (Fig. 1) whereas the distance between hydrogen bonded neighboring strands is ~4.7–4.8 Å. These dimensions allow a rough estimation of the area occupied by peptides in the β-pleated conformation at interfaces (i.e. 3.45 × 4.75 × number of residues).

A set of peptides designed to assume 2-D ordered assemblies at interfaces have been studied by GIXD at air–water interfaces [17]. These peptides could be represented by the generic sequence X − Y − (Z − Y)*n* − X, where the N- and C-terminal residues (X) bear charged ammonium and carboxylate groups, respectively, and Y and Z are alternating hydrophilic and hydrophobic amino acids. Variations in amino acid sequence and in the number of dyads (*n*) participating in hydrogen-bond formation were expected to tune the intermolecular interactions and therefore the dimensions of the 2-D ordered β-sheet domains. The 2-D order was expected to be enhanced by choosing the termini amino acids (X) to be proline (Pro), a potent breaker of α-helix and β-sheet structures.

Grazing-incidence X-ray diffraction (GIXD) experiments on Pro–Glu–$(Phe–Glu)_4$–Pro Langmuir films on water provided clear evidence for assembly of the peptide into 2-D crystalline β-sheet monolayers [17]. A peak corresponding to 4.7 Å spacing was attributed to pleated peptide strands interlinked by N–H···O = C hydrogen bonds. A Bragg peak corresponding to 37.4 Å was also obtained and assigned to the repeat distance defined by juxtaposition of neighboring hydrogen-bonded ribbons (Fig. 1b–c). The full widths at half-maxima of GIXD Bragg rods indicated a crystalline film ~8 Å thick, implying that

not only the peptide backbone was ordered but also part of the amino acid side chains that extended above and below the peptide backbone plane. FTIR-ATR spectrum of a Pro–Glu–$(Phe–Glu)_4$–Pro monolayer, transferred from the air–water interface to a ZnSe crystal, displayed amide I absorption bands at 1630 and 1694 cm^{-1} and an amide II band at 1540 cm^{-1} characteristic of the antiparallel β-sheet structure. In particular, the weak 1694 cm^{-1} band constitutes strong evidence for the antiparallel structure, as it has been detected for crystals with the antiparallel β-sheet motif but not for the parallel arrangement. The two 11 residues peptides, $(Phe–Glu)_5$–Phe and Pro–Glu–$(Phe–Glu)_4$–Pro, would have been expected to yield similar diffraction patterns, if adopting at the air water interface, similar packing arrangements. Nonetheless, $(Phe–Glu)_5$–Phe exhibited a very weak Bragg peak corresponding to the spacing along the peptide long axis, along *b* (Fig. 1), in contrast to a strong peak that was observed for Pro–Glu–$(Phe–Glu)_4$–Pro. Structure factor calculations for $(Phe–Glu)_5$–Phe showed that offsets in peptide registry along the *b* axis in steps of ca. 6.9 Å (the intramolecular repeat distance between amino acids of the same type), strongly diminished the intensity of that peak. Therefore, peptide $(Phe–Glu)_5$–Phe which lacks the distinct Pro termini residues, exhibited extensive dislocation defects along the *b* direction of the sort shown schematically in Fig. 1a.

Recently, Pro termini have been found to effectively induce the formation of peptide nanofibers with homogeneous morphology [18]. Water soluble amphiphilic β-sheet peptides were designed as sequences of Pro–Lys–X1–Lys–X2–X2–Glu–X1–Glu–Pro with X1 and X2 being hydrophobic residues selected from Phe, Ile, Val, or Tyr. The peptide FI (X1 = Phe; X2 = Ile) self-assembled into straight fibers with 80 ± 120 nm widths and clear edges, as revealed by transmission electron microscopy (TEM) and by AFM. The peptides with X1 = X2 = Phe formed fibers in a hierarchical manner. It has been suggested that the assembly of peptide FI is initiated by β-sheet peptides forming a protofibril. The protofibrils assemble side-by-side to form a ribbon and the ribbons then coil in a left handed fashion to make up a straight fiber. In contrast, a peptide with Ala residues at both N and C termini did not form fibers with clear edges but rather aggregated into relatively small pieces of fibers. Both the above-mentioned studies of Pro terminated peptides at interfaces and in solution demonstrated the potential effect of unique peptide termini on the extent of order of peptide assemblies (Fig. 2).

Flat β-sheet structures as those obtained at the air–water interface are not common in globular proteins. In globular proteins twisted β-sheets represent a lower energy conformation of the polypeptide chain [19].

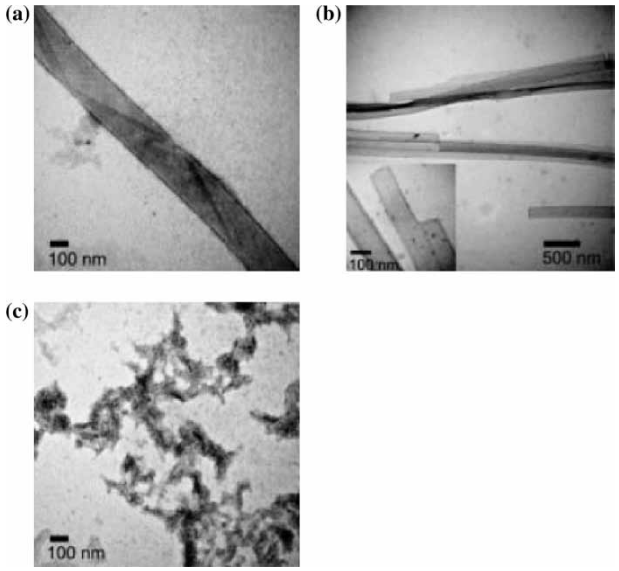

FIGURE 2 TEM images of Pro–Lys–X1–Lys–X2–X2–Glu–X1–Glu–Pro with a) fiber of the X1 = X2 = Phe peptide assemblies, exhibiting a large width and clear edges; b) fibers of the peptide X1 = Val and X2 = Ile that do not coil. These tape-like fibers associate side-by-side into fibers of variable width. The inset shows no crossed striations in the tape-like fibers; c) image of fibers formed from peptide similar in sequence to that shown in (a) but with Ala termini residues instead of Pro, showing disordered aggregation of small pieces. Reprinted with permission from ref. [18]. (Copyright 2004 Wiley-VCH.)

Nonetheless, the systems discussed above and other fibrous proteins [10,20], do exhibit flat sheets mainly, as a result of specific amino-acid sequences. Recently it has been demonstrated that interfaces may induce the formation of flat cross-β assemblies in peptides that otherwise, in solutions, form twisted tape-like assemblies [21]. The peptide CH3CO–Gln–Gln–Arg–Phe–Gln–Trp–Gln–Phe–Glu–Gln–Gln–CONH2 (P_{11}-2) assembles in solution, in a hierarchical manner, into cross-β tape-like structure which further associate into ribbons (double tapes), fibrils (stacks of four or more tapes), and fibers (entwined fibrils). This hierarchical self-assembly behavior has been attributed to the chirality of the individual peptide molecules [22]. Recently Whitehouse *et al*. studied the adsorption and self-assembly, of P_{11}-2 peptide [23], on solution/mica interface. These studies were performed at concentrations below the critical tape concentration (ca. 90 μm) in order to reveal specifically, the interfacial assemblies and to avoid formation of the tape-like aggregates in solution. Their hypothesis was that below the critical tape concentration, planar tape-like structures could self-assemble at solid/solution interfaces, provided the peptide/surface binding energy is more than sufficient to compensate for the elastic distortion energy cost of "flattening" the tape onto the surface. P_{11}-2 did not adsorb on mica from water solution. However, by using a solvent composed of a mixture of 10% water in 2-propanol (v/v), with a dielectric constant 26.1 that is lower than that of water (80), the adsorption of the peptide onto the mica

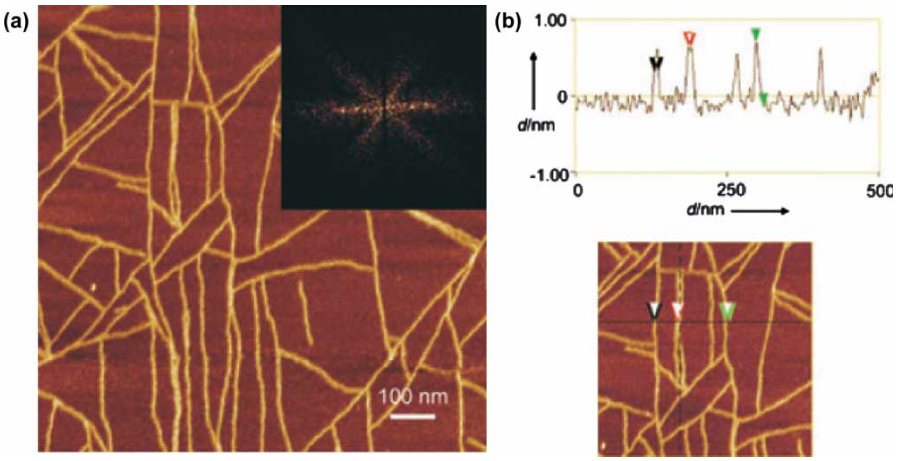

FIGURE 3 In situ AFM images measured by the tapping mode showing single β-sheet tapes grown on mica from 5 μM P_{11}-2 in 10% H_2O in 2-propanol; height scale 2 nm. a) Tapes aligned with the hexagonal symmetry of the underlying mica lattice with Fourier transform of the image showing hexagonal symmetry (inset, top right corner). b) Section analysis with line graph (top) showing the width (black arrows, convoluted width 6.9 nm) and height (green arrows, 0.8 nm) of the self-assembled tapes. The red arrows show the peak-to-peak distance (4.9 nm) between adjacent tapes. Reprinted with permission from ref. [21]. (Copyright 2005 Wiley-VCH.) (The colour version of this figure is included in the online version of the journal.)

surface was induced. Under these conditions AFM images revealed the spontaneous formation of β-sheet tapes at the surface of the mica substrate in solution (Fig. 3). The peptide tapes appeared to grow epitaxially to produce a two-dimensional network that reflected the hexagonal symmetry of the mica surface lattice. The peak-to-peak distance between two touching tapes was 49 Å, and the width of a tape was 69 Å. Both these dimensions are longer than the estimated length of an 11-residue peptide in an extended β-strand conformation that is ~38 Å (~3.45 × 11). The distances detected by the AFM measurement, may suggest that P_{11}-2 elongated assemblies were composed of two neighboring flat tapes, a packing that could possibly be facilitated by hydrogen bonds between peptide amide termini.

SINGLE STRANDED PARALLEL β-SHEETS

The effect of specific amino acid sequences on the assembly of β-sheet peptides was demonstrated in a system designed to exhibit parallel β-sheets at interfaces. In β-sheet assemblies, the nearest neighbor amino acids are situated 4.7–4.8 Å apart, on neighboring strands that are interlinked by C═O···H–N hydrogen bonds. Neighboring amino acids along a strand, which point to the same face of the sheet are ~6.9 Å apart. Accordingly, interactions between cross-strand amino acid pairs may be stronger than those between intrastrand neighboring residue pairs. Indeed, stabilizing cross-strand pair interactions, as for example, between the oppositely charged residues Glu–Lys and Glu–Arg or between aromatic side chains Phe–Phe, are ubiquitous in the β-sheet regions of natural proteins [24].

Energy minimization calculations [25], experimental studies [26] and simple dipole moment considerations suggest that the antiparallel packing mode of β-strands is more favorable than that of the parallel. Recently, the possibility of inducing parallel β-sheet assembly by specific cross-strand pair electrostatic interactions was explored [27]. The experimental system included two amphiphilic peptides, P_A and P_B, identical in sequence but for the two amino acids, Lys and Glu, reversed in positions along the strands.

P_A: CH_3CO–Pro–Cys–Phe–Ser–Phe–Lys–Phe–Glu–Pro–NH_2
P_B: CH_3CO–Pro–Cys–Phe–Ser–Phe–Glu–Phe–Lys–Pro–NH_2

Two cross-strand pair interactions between the oppositely charged Glu and Lys residues were expected to support the hydrogen-bonded parallel arrangement of neighboring P_A and P_B peptides at air–water interfaces.

All three studied systems, i.e. each of the peptides and their equimolar ratio mixture, were found by FTIR measurements to pack in the parallel arrangement. AFM topography scans of the peptide monolayers that were transferred to mica support (Fig. 4) revealed substantial differences in the assembly patterns of all three studied systems. GIXD measurements indicated the formation of 2-D ordered assemblies by peptide P_B monolayer at the-water interface with a 4.77 Å between hydrogen bonded strands and an additional 39.5 Å spacing along the peptide backbone direction. This spacing which is larger than the estimated length of the nine-residue peptide (~31 Å) was rationalized by a model that incorporates a 6.9 Å offset (along the β strands axes direction) between neighboring parallel P_B strands

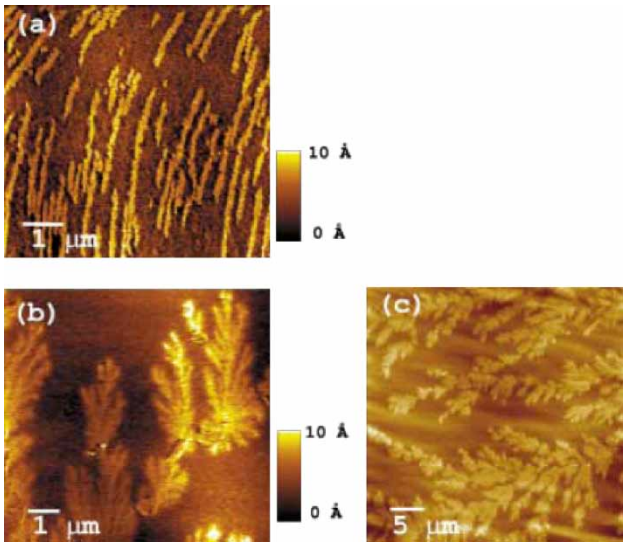

FIGURE 4 AFM topography images of monolayers deposited on mica. (A) P_B assemblies showing tapes stretched along the same direction (B–C) The equimolar ratio film of P_A P_B showing fractal-like structures in both images. P_A peptide film (not shown) exhibited non uniform aggregates. Reprinted with permission from ref. [27]. (Copyright 2004 Wiley-VCH.)

(Fig. 5). In such an assembly the Glu and the Lys of neighboring P_B (along the 4.77 Å spacing) may form cross-strand pairs. Disulfide bridge formation, leading to molecular mass doubling, was detected by mass spectrometry only for the P_A and P_B equimolar ration mixture.

DOUBLE STRANDED β-SHEET PEPTIDES

Amphiphilic peptides **1** and **2** that fold into β-hairpin structure were designed by Powers and Kelly [28]. The folded conformation was induced by the D-Pro–Gly, type II′ β-turn. The peptides comprised alternating hydrophilic (Glu) and hydrophobic (Nle or Val) amino acids that induce β-strand conformation at the air–water interface. The peptides were labeled with the 5,7-dimethyl derivative of the BODIPY fluorophore (DMBDY) to enabled fluorescence microscopy measurements. Peptide **1** was shown to form monolayers on the surface of water either by spreading from a volatile organic solution or by adsorption from an aqueous solution. The fluorescence studies have shown that in adsorbed monolayers of peptide **1** the shape and type of domains are dominated by dynamic events; depending on the conditions, islands of peptide in the two-dimensional liquid or solid phase were detected.

2

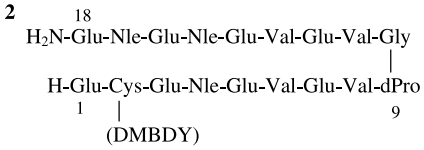

1

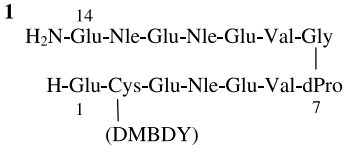

Single layer LB films of peptides **1** and **2** were deposited at 10 mN/m onto freshly cleaved mica. The Langmuir-Blodgett (LB) monolayers were imaged by tapping mode AFM [29] (Fig. 6) using single-wall carbon nanotube (SWNT) tips, which have better reproducibility and higher resolution compared to Si tips. The peptide monolayers exhibited well-ordered molecular arrays with individual domains extending for hundreds of nanometers in monolayers of **1** and

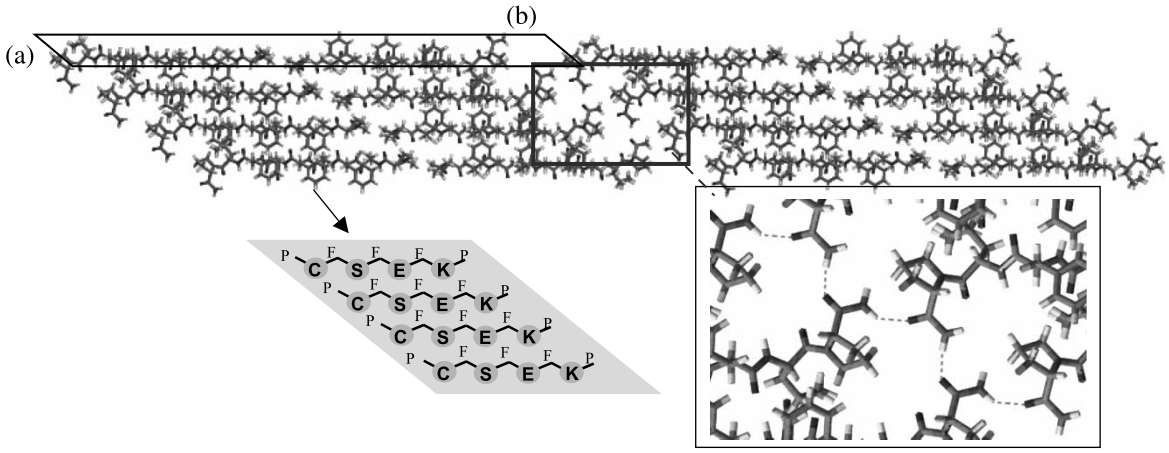

FIGURE 5 Proposed molecular model (view orthogonal to the *ab* plane) of the two-dimensional packing arrangement of peptide P_B unit cell, in *p*2 symmetry, but for amides C-termini relaxed to allow hydrogen bonding. The unit cell (line) yields an (0,1) spacing that matches the observed 39.5 Å spacing. Bottom-right: Enlarged view (orthogonal to the *ab* plane) of possible interstrand hydrogen bond network along the *a* axis. Bottom-left: Schematic representation of P_B strands along the *a* axis, peptide backbone (line), amino acids side chains designated by the one letter code, hydrophilic amino acids marked by gray circles (view orthogonal to the *ab* plane). Reprinted with permission from ref. [27]. (Copyright 2004 Wiley-VCH.)

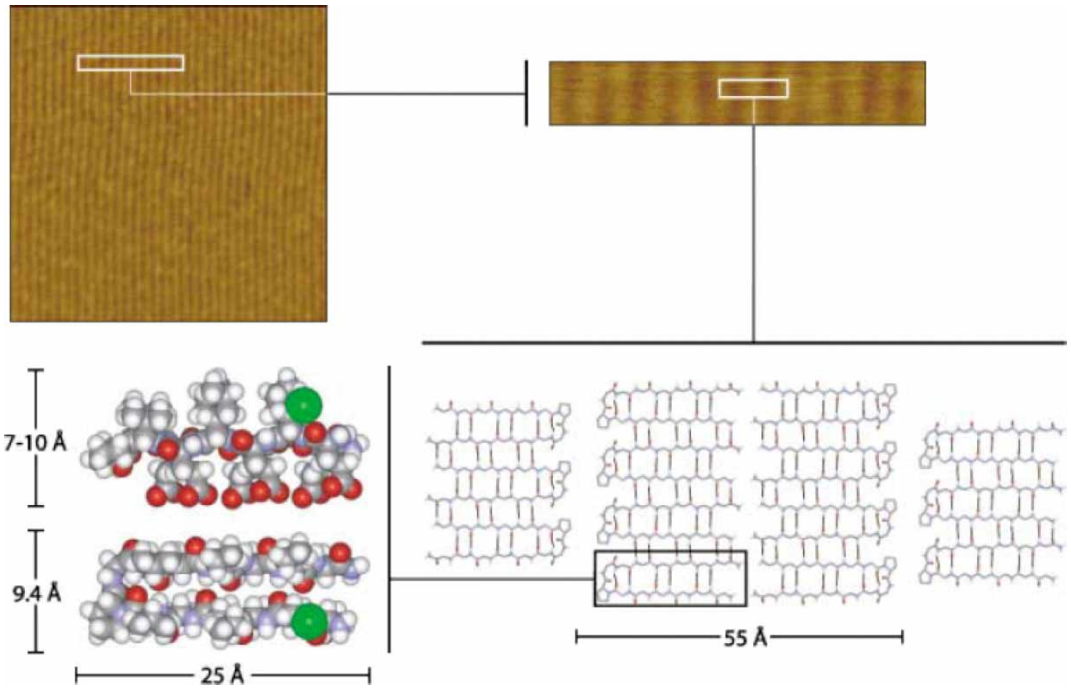

FIGURE 6 Molecular model for the assembly of ***1***. The area scanned by AFM, top left. A white box encloses a small section of the scan area, which is expanded in the top right. Another white box in the expansion encloses a ridge with two flanking half-ridges. A molecular model for the assembly in the enclosed area is shown in the bottom right. The central ridge corresponds to the two central columns of β-hairpins, which interact with each other through their polar termini. The flanking half-ridges correspond to the two flanking columns of β-hairpins, which interact with the central column through turn–turn recognition. The ridge period expected from this model is 55 Å: 25.0 Å for each hairpin, 2 Å for the gap at the termini-to-termini interface (a typical distance for hydrogen bonds), and 3 Å for the gap at the turn-to-turn interface (a typical distance for van der Waals interactions). The panel in the bottom left shows a top view (lower part of panel) and a side view (upper part) of a single hairpin. The hairpin's length is 25 Å and its width is 9.4 Å (see top view), while its height can be from 7 to 10 Å depending on the side chains conformations (see side view). The green spheres represent the DMBDY fluorophore. Reprinted with permission from ref. [29]. (Copyright 2002 Wiley-VCH.)

tens of nanometers in monolayers of **2**. The observed ridges were 59(±1) Å for **1** and 74(±1) Å for **2**. The structural model of peptide **1** shown in Fig. 6 was based also on previous measurements of peptide **1** at interfaces. The 9.4 Å spacing shown in the model, between neighboring hairpins along the β-sheet interstrand hydrogen bonds, was beyond the resolution limit of the AFM measurements. Nevertheless, this spacing relies on previously performed FTIR measurements [28] which indicated high β-sheet content in the antiparallel mode. The length of peptide **1** in the β-hairpin conformation is ~25 Å (i.e. ~3.45 × 7 without considering the length added by the β-turn). The registered tapes detected by the AFM were 59(±1) Å, strongly suggesting that the observed ridges correspond to the length of two neighboring hairpin peptides. The assembly into tapes that are two hairpin peptides wide, was attributed to the two different termini of the hairpin peptides: a polar one composed of the charged amine and the C-amide termini and a nonpolar one composed of the turns. The model suggested exhibits hairpin peptides assembled such that the hydrophilic and hydrophobic termini are segregated to opposite sides generating individual ridges that correspond to pairs of cross-β sheets of 55 Å, within 7% of the observed 59(±1) Å. The expected monolayer height in this model is 7–10 Å depending on the side chain conformations that matched well the 7 Å height measured by AFM.

These studies also demonstrated that longer peptides, with larger lattice spacing, exhibit decreased monolayer order. The same trend has been found in GIXD characterization of peptide's 2D ordered Langmuir films [17]. The correspondence between the results obtained for peptide monolayers at the air/water interface and for peptides on mica suggest that in general, the β-sheet assemblies may withstand the Langmuir–Blodgett (LB) transfer from the air/water interface onto the mica surface and that the corresponding AFM images indeed reflected the LB film state and degree of order.

Neutron reflection studies have been applied on peptide ***1*** monolayer that was obtained by adsorption from solution [30]. Based on neutron reflectivity models the scattering data indicated increase in film thickness (from 8 ± 3 to 11 ± 2 upon increase from 0.38 to 3.8 μg/ml, respectively, in peptide solution concentration) that also manifested in increase in surface pressure [28]. The authors suggested that the change in thickness indicated responsive variation in amino acids side chain conformations that is dependent on the surface area per peptide. These neutron

reflectivity measurements also indicated that the peptide monolayer is predominantly afloat on the surface of water, with the carboxylic groups hydrated only.

MULTI-STRANDED β-SHEET PEPTIDES AT INTERFACES

The 30-residue peptide BS30 was designed to fold into the triple-stranded β-sheet at hydrophilic–hydrophobic interfaces [31], as depicted schematically in Fig. 7. This molecular architecture has been suggested to depend on formation of two reverse turns, and on proper registry of the alternating hydrophilic and hydrophobic amino acids along the peptide three strands. These amphiphilic strands were designed to extend along the plane of the interface, in an arrangement that is unlikely to occur in globular proteins, where neighboring strands are twisted relative to one another [19]. The inclusion of D-Pro in type II′ β-turn has been described above for the hairpin amphiphilic peptides designed by Powers and Kelly [28–30]. As for the BS30 system, the authors preferred to utilize a β-turn motif with natural L- configuration amino-acids. The L-Pro is the most abundant amino acid to occupy position i + 1 in type II β-turns [32]. This type of turn however, rarely appears in natural proteins since it does not support the twist between neighboring β-strands. Nevertheless, since the triple-stranded peptide BS30, was designed to assume a flat shape at the air–water interface, with strands lying parallel to the air–water interface, it was finally designed with a type II β-turn with L-Pro at position i + 1. By analogy with the previously designed single-stranded amphiphilic β-sheet peptides [17], Phe and Glu were selected as the alternating hydrophobic and hydrophilic amino acids along the strands. Two Leu residues were placed adjacent to one of the β-turns to provide greater conformational flexibility (compared to that from Phe) and to impose fewer steric restrictions in the region close to the turn (the other turn in the peptide is next to Glu residues that appeared not to impose structural restrictions according to molecular models).

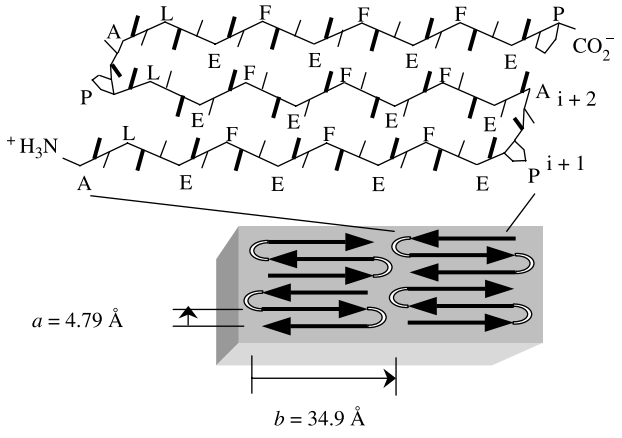

FIGURE 7 Schematic representation of the triple stranded peptide BS30 (top) and possible assembly at a hydrophilic interface (bottom) showing peptide backbone (line), carbonyl and amine groups (thick and thin lines, respectively). Amino acid side chains are assigned by one letter code; two amino acids in the turn are designated as the $i + 1$ and $i + 2$ residues of a β-hairpin motif. Reprinted with permission from ref. [31]. (Copyright 2002 American Chemical Society.)

Surface pressure versus molecular area isotherms of BS30 indicated a limiting area per molecule ~460 Å^2 that corresponds reasonably well to 492 Å^2 estimated from the known dimensions of crystalline β-sheet monolayers (~3.45 × 4.75 × 30). ATR-FTIR measurements of BS30 monolayer films transferred by the Langmuir–Schaffer method onto ZnSe prism, indicated the formation of antiparallel β-sheet structure. GIXD measurements performed on the BS30 monolayer at nominal area per molecule of 500 Å^2, revealed Bragg peaks that correspond to spacings of 34.9 and 4.79 Å. The 4.79 Å spacing, is the characteristic β-sheet interstrand spacing and the 34.9 Å could be attributed to the repeat distance of juxtaposed neighboring triple stranded peptides (along b, Fig. 7). The full width at half-maximum of each of the two Bragg peaks indicated crystalline coherence lengths along the *a* and *b* directions (Fig. 7) of about 250 Å. The full width at half-maxima of the Bragg rods indicated a film thickness of ~9 Å, in good agreement with the single stranded β-sheet systems described above [17].

Hecht *et al*. developed a biomimetic system, which utilized the highly ordered surface of HOPG to template the assembly of a *de novo* designed β-sheet protein [33]. The protein used in this study, 17-6, was chosen from a combinatorial library of amino acid sequences designed *de novo* to form β-sheet proteins [34,35]. The library design specified that each protein should contain 6 β-strands, and each β-strand would be 7 residues long, with polar and nonpolar amino acids arranged in an alternating pattern (Fig. 8). Combinatorial diversity was incorporated into the library of the proteins by allowing polar residues to be His, Lys, Asn, Asp, Gln, or Glu; and nonpolar residues to be Leu, Ile, Val, or Phe [34]. These combinatorial sets of amino acids were encoded by libraries of synthetic genes with polar residues specified by the degenerate DNA codon VAS, and nonpolar residues by the degenerate DNA codon NTC (where V = A, G, or C; S = G or C; and N = A, G, C, or T). The proteins in this library have a total length of 63 residues including six β-strands with seven residues per strand and five intervening turns, each with four residues.

A solution of protein 17-6 was deposited onto freshly cleaved HOPG, and the resulting assemblies were imaged with tapping mode AFM (Fig. 9). The protein assembled into parallel fibers on the HOPG

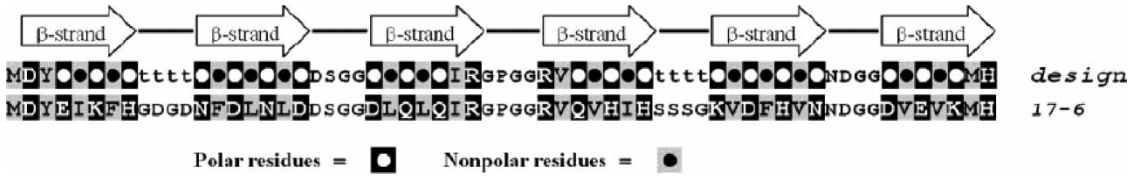

FIGURE 8 Polar/nonpolar ("binary"') patterning of designed β-sheet proteins. β-Strands are shown as arrows. Polar residues are in white font on black background, and nonpolar residues are in black font on gray background. Combinatorial diversity was incorporated in the original library [34] at positions marked O, b, and t (turn). The amino acid sequence of protein 17-6 is shown in the single letter code. Reprinted with permission from ref. [33]. (Copyright 2002 American Chemical Society.)

surface showing three preferred orientations at 120° to each other. This symmetry indicated that the hexagonal lattice of graphite directed the nucleation of the fibers. The straightness of the fibers and their persistence length of several microns suggested that the template also influenced the addition of protein monomers onto the growing fiber. FTIR measurement were performed of 17-6 protein in a procedure that ensured the monomeric form of the protein before the assembly: a 15 microliter drop (3 mg/mL) was placed on preheated ZnSe prism that was allowed to cool in a controlled manner. The resultant film exhibited absorption bands typical of antiparallel β-sheet assemblies [33]. The width of a cross-β structure, as estimated from the known geometry has been estimated to be ~34 Å (i.e. strand lengths of ~24 Å = ~3.45 × 7 plus ~ 5 Å per turns on either side of the cross β-structure). According to the AFM images the apparent width of each fiber was ~200 Å. The authors explained the discrepancy between the estimated width of the cross-β structure and that observed by AFM, by the effect of the nonzero diameter of the AFM tips. Their calculations which take into account the tip diameter, yielded an estimated width of ~40 Å that is consistent with the estimation of ~34 Å.

Noteworthy, GIXD measurements have been utilized for the study of naturally occurring β-sheet systems such as amyloid beta-peptides and antimicrobial peptides. The amyloid peptides that were studied by GIXD at air–aqueous solution interfaces were 40 residues long. In two different studies, Bragg peaks corresponding to two dimensional order of these peptides at the air–water interface have been obtained [36,37]. However, a molecular model for the interfacial ordering of the amyloid peptide, which could account for the diffraction data, is yet to be elucidated. The effect of the naturally occurring β-sheet antimicrobial peptide protegrin-1 (PG-1), on phopholipid Langmuir film was also investigated by

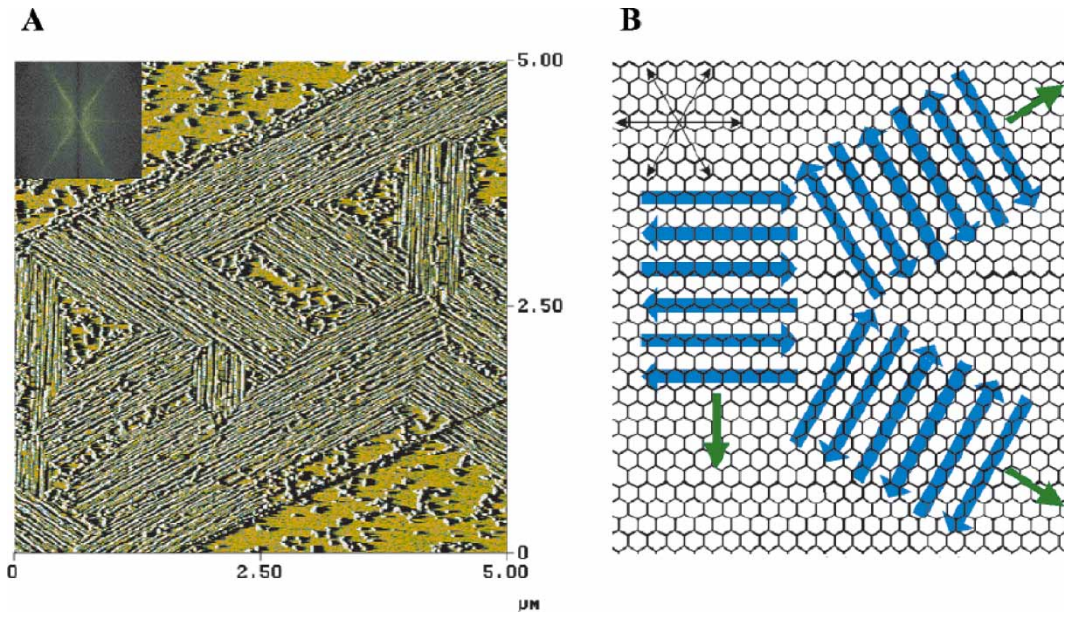

FIGURE 9 (A) AFM image of protein 17-6 deposited on highly ordered pyrolytic graphite (HOPG). The inset shows a Fourier transform of this image. The 3-fold symmetry is apparent both in the AFM image and in its Fourier transform. The adsorbed protein was imaged under ambient conditions by using tapping mode AFM. The globular deposits on the graphite likely consist of nonordered aggregates of the protein. The image was collected in amplitude mode. Data collected in height mode showed the same features. (B) Schematic representation of a 6-stranded β-sheet protein assembled on a HOPG surface. β-Strands are shown as blue arrows. The 3-fold symmetry of the graphite template is recapitulated in the assembly of the protein. The long axis of the fibers (part A) is perpendicular to the β-strands and is indicated with green arrows. The relative orientation of the fibers to the graphite lattice was determined by imaging a sample of fibers and subsequently imaging the graphite lattice underneath the fibers by using contact mode AFM. Reprinted with permission from ref. [33]. (Copyright 2002 American Chemical Society.)

GIXD [38]. PG-1 is an18 residues, amidated peptide (NH2-RGGRLCYCRRRFCVCVGRCONH2) originally isolated from porcine leukocytes. According to NMR studies PG-1 adopts a one-turn β-hairpin structure stabilized by two disulfide bonds. The GIXD experiments demonstrated that the insertion of PG-1 into the phospholipid monolayer disrupted the phospholipid ordering.

ORDERED AMPHIPHILIC HELICAL ASSEMBLIES

Alamethicin is a hydrophobic α-helical peptide antibiotic that forms voltage-gated ion channels in lipid membranes. It is made up of 19 amino acid residues and one amino alcohol in the following sequence:

$$\text{Ac–Aib–}\overset{1}{\text{Pro}}\text{–Aib–Ala–Aib–Ala–Gln–Aib–Val–}\overset{10}{\text{Aib}}\text{–Gly–Leu–Aib–Pro–Val–Aib–Aib–Glu–Gln–}\overset{20}{\text{Phol}}$$

where Aib denotes α-aminoisobutyric acid, and Phol denotes phenylalaninol. Alamethicin folds into a helical structure with estimated cross-section areas of 320 $Å^2$ and 80 $Å^2$, parallel and perpendicular to the helix axis, respectively. The helical peptide exhibits amphipaticity with the polar hydrophilic groups, Gln7, Glu18, Gln19, and Phol20 lying along a narrow strip parallel to the helix axis. The majority of the other amino acid residues, including the N terminus, are hydrophobic in nature. The structural organization of alamethicin at the air–water interface was studied by Langmuir monolayers and by GIXD [39]. The Langmuir isotherm of alamethicin demonstrated that it forms stable monolayers at the air/water interface composed of helices oriented with their helix axis parallel to the air–water interface. The other possibility of helices oriented with their axes normal to the interface was excluded since the collapse" region of alamethicin extended down to zero molecular areas, indicating no transition at area per molecule (80 $Å^2$) that corresponds to helices oriented normal to the interface. Grazing incidence X-ray diffraction measurements, acquired at a surface pressure of 20 mN/m, provided a diffraction pattern which was attributed to helices packed in a pseudo-rectangular lattice, with lattice parameters $a = 9.635$ Å, $b = 33.89$ Å and an angle between the vectors a and b of $\gamma = 93.87°$. The values of the b and a axes correspond to the helix length and diameter respectively and the area per molecule in the lattice, 326 $Å^2$ corresponds well with the limiting area per molecule obtained by surface-pressure area isotherm. According to FWHM of the Bragg peaks the ordered domains extended to ~80 helices, packed side by side (along the a axis) and ~16 in the direction parallel to the helix long axis (along the β axis).

Beyond the study of the natural compound of alamethicin at the air–water interface there have not been other reported GIXD studies of helical peptide systems, which packed into two-dimensional ordered assemblies. Other studies have attempted to form ordered assemblies composed of polypeptides, tens to more than a hundred amino acids long. The group of Kinoshita *et al.* utilized Langmuir–Blodgett methods to generate assemblies composed of amphiphilic polymers of di- and triblock helical copolypeptides at interfaces [40]. High resolution AFM scans of polypeptide films on mica-support revealed local order, extending only to tens of nanometers, formed by rod-like helices lying with their long axes parallel to the interface. The authors suggested that the molecular order of such polypeptide assemblies could be extended by monodispersed polypeptide systems. Noteworthy, the monodisperse poly(γ-benzyl L-glutamate) (PBLG) has been shown by Yu, Tirrell *et al.* [11] to form, both in bulk solutions and solution cast films, a smectic-like liquid crystalline order composed of helical rods. The study of the same system in Langmuir film at the air–water interface by GIXD indicated only nematic-like, limited one-dimensional order [41]. The authors suggested that the smectic ordering in the bulk was achieved by inhibition of PBLG aggregation whereas the film preparation at the air–water interface did not suppress the local aggregation of PBLG molecules and that lead to glassy planar domains.

SUMMARY AND OUTLOOK

Various factors have been shown in this review to affect, at the molecular level, the manner in which peptide self-assemble at interfaces. The amino acid sequence strongly affects the peptide secondary structure and its assembly forms. The examples illustrated herein demonstrate the progress in understanding β-sheet amphiphilic structures at interfaces through rationally designed sequences and rigorous GIXD or AFM structural characterizations. Most of these peptides were designed down to every amino acid in the sequence and the experimental results confirmed the targeted morphology. Indeed, more efforts need to be invested in controlling the size of the ordered assemblies

and avoiding structural defects. The studies presented herein, share a few common characteristics. All the β-sheet systems discussed above constitute strands with the pattern of alternating hydrophobic and hydrophilic amino acids. The planar multi-stranded β-sheets were designed both with type II and type II′ β-turns, with the L-Pro and D-Pro respectively, inducing these specific turns. It is yet to be determined which of these turns is energetically more preferable for the multi-stranded β-sheet structure. The six-stranded β-sheet system suggests that appropriately controlled assembly conditions and solid interfaces have greater effect, than the specific turn amino acids, on the formation of a multi-stranded β-sheet structure. In contrast to the various β-sheet peptides studied and the accumulating data on typical assembly dimensions and factors affecting them, to date there has been only one helical peptide system shown by GIXD, to organize into ordered two-dimensional assemblies. In summary, the recent achievements in controlling the assembly of versatile peptides at interfaces are expected to foster further along with the growing interest in nanometer-scale functional materials.

References

[1] Lehn, J.-M. *Science* **2002**, *295*, 2400.
[2] Gale, P. A. *Phil. Trans. R. Soc. Lond. A* **2000**, *358*, 431.
[3] Malcolm, B. R. In *Progress in Surface and Membrane Science, Vol.7*; Danielli, J. F., Rosenberg, M. D., Cadenhead, D. A., Eds. Academic Press: New York, 1973.
[4] Brack, A.; Caille, A. *Int. J. Peptide Res.* **1978**, *11*, 128.
[5] Pierre, S. S.; Ingwall, R. T.; Verlander, M. S.; Goodman, M. *Biopolymers* **1978**, *17*, 1837.
[6] Kaiser, E. T.; Kezdy, F. J. *Proc. Natl. Acad. Sci. USA — Phts. Sci.* **1983**, *80*, 1137.
[7] Osterman, D.; Mora, R.; Kezdy, F. J.; Kaiser, E. T.; Meredith, S. C. *J. Am. Chem. Soc.* **1984**, *106*, 6845.
[8] DeGrado, W. F.; Lear, J. D. *J. Am. Chem. Soc.* **1985**, *107*, 7684.
[9] Rapaport, H.; Kuzmenko, I.; Berfeld, M.; Kjaer, K.; Als-Nielsen, J.; Popovitz-Biro, R.; Weissbuch, I.; Lahav, M.; Leiserowitz, L. *J. Phys. Chem. B.* **2000**, *104*, 1399.
[10] Krejchi, M. T.; Atkins, E. D. T.; Waddon, A. J.; Fournier, M. J.; Mason, T. L.; Tirrell, D. A. *Science* **1994**, *265*, 1427.
[11] Yu, S. M.; Conticello, V. P.; Zhang, G.; Kayser, C.; Fournier, M. J.; Mason, T. L.; Tirrell, D. A. *Nature* **1997**, *389*, 167.
[12] Zhang, S. G.; Yan, L.; Altman, M.; Lassle, M.; Nugent, H.; Frankel, F.; Lauffenburger, D. A.; Whitesides, G. M.; Rich, A. *Biomaterials* **1999**, *20*, 1213.
[13] Steinem, C.; Janshoff, A.; Vollmer, M. S.; Ghadiri, M. R. *Langmuir* **1999**, *15*, 395.
[14] Horne, W. S.; Ashkenasy, N.; Ghadiri, M. R. *Chem. Eur. J.* **2005**, *11*, 1137.
[15] Bekele, H.; Fendler, J. H.; Kelly, J. W. *J. Am. Chem. Soc.* **1999**, *121*, 7266.
[16] Cavalli, S.; Popescu, D. C.; Tellers, E. E.; Vos, M. R. J.; Pichon, B. P.; Overhand, M.; Rapaport, H.; Sommerdijk, N. A. J. M.; Kros, A. *Angew. Chem. Int. Ed.* in press **2005**.
[17] Rapaport, H.; Kjaer, K.; Jensen, T. R.; Leiserowitz, L.; Tirrell, D. A. *J. Am. Chem. Soc.* **2000**, *122*, 12523.
[18] Matsumura, S.; Uemura, S.; Mihara, H. *Chem. Eur. J.* **2004**, *10*, 2789.
[19] Chothia, C. *J. Mol. Biol.* **1973**, *75*, 295.
[20] Krejchi, M. T.; Cooper, S. J.; Deguchi, Y.; Atkins, E. D. T.; Fournier, M. J.; Mason, T. L.; Tirrell, D. A. *Macromolecules* **1997**, *30*, 5012.
[21] Whitehouse, C.; Fang, J.; Aggeli, A.; Bell, M.; Brydson, R.; Fishwick, C. W. G.; Henderson, J. R.; Knobler, C. M.; Owens, R. W.; Thomson, N. H.; Alastair Smith, D.; Boden, N. *Angew. Chem. Int. Ed.* **2005**, *44*, 1965.
[22] Aggeli, A.; Nyrkova, I. A.; Bell, M.; Harding, R.; Carrick, L.; McLeish, T. C. B.; Semenov, A. N.; Boden, N. *Proc. Natl. Acad. Sci. USA* **2001**, *98*, 11857.
[23] Aggeli, A.; Bell, M.; Boden, N.; Keen, J. N.; McLeish, T. C. B.; Nyrkova, I.; Radford, S. E.; Semenov, A. *J. Mater. Chem.* **1997**, *7*, 1135.
[24] Smith, C. K.; Regan, L. *Science* **1995**, *270*, 980.
[25] Chou, K. C.; Nemethy, G.; Scheraga, H. A. *Biochemistry* **1983**, *22*, 6213.
[26] Kobayashi, K.; Ghadiri, M. R. *Angew. Chem. Int. Ed.* **1995**, *34*, 95.
[27] Sneer, R.; Weygand, M. J.; Kjaer, K.; Tirrell, D. A.; Rapaport, H. *Chem. Phys. Chem.* **2004**, *5*, 747.
[28] Powers, E. T.; Kelly, J. W. *J. Am. Chem. Soc.* **2001**, *123*, 775.
[29] Powers, E. T.; Yang, S. I.; Lieber, C. M.; Kelly, J. W. *Angew. Che. Int. Ed.* **2002**, *41*, 127.
[30] Lu, J. R.; Perumal, S.; Powers, E. T.; Kelly, J. W.; Webster, J. R. P.; Penfold, J. *J. Am. Chem. Soc.* **2003**, *125*, 3751.
[31] Rapaport, H.; Kjaer, K.; Jensen, T. R.; Moller, G.; Knobler, C.; Leiserowitz, L.; Tirrell, D. A. *J. Am. Chem. Soc.* **2002**, *124*, 9342.
[32] Hutchinson, E. G.; Thornton, J. M. *Protein Science* **1994**, *3*, 2207.
[33] Brown, C. L.; Aksay, I. A.; Saville, D. A.; Hecht, M. H. *J. Am. Chem. Soc.* **2002**, *124*, 6846.
[34] West, M. W.; Wang, W.; Patterson, J.; Mancias, J. D.; Beasley, J. R.; Hecht, M. H. *Proc. Natl Acad. Sci. U.S.A.* **1999**, *96*, 11211.
[35] Xu, G.; Wang, W.; Groves, J. T.; Hecht, M. H. *Proc. Natl. Acad. Sci. USA* **2001**, *98*, 3652.
[36] Ege, C.; Majewski, J.; Wu, G.; Kjaer, K.; Lee, K. Y. C. *Chem. Phys. Chem.* **2005**, *6*, 226.
[37] Maltseva, E.; Kerth, A.; Blume, A.; Mohwald, H.; Brezesinski, G. *Chem. Bio. Chem.* **2005**, *6*, 1817.
[38] Gidalevitz, D. Y.; Ishitsuka, Y.; Muresan, A. S.; Konovalov, O.; Waring, A. J.; Lehrer, R. I.; Lee, K. Y. C. *Proc. Natl Acad. Sci. U.S.A.* **2003**, 100.
[39] Ionov, R.; El-Abed, A.; Angelova, A.; Goldmann, M.; Peretti, P. *Biophys. J.* **2000**, *78*, 3026.
[40] Niwa, T.; Yokoi, H.; Kinoshita, T.; Zhang, S. *Polymer J.* **2004**, *36*, 665.
[41] Fukuto, M.; Heilman, R. K.; Pershan, P. S.; Yu, S. M.; Griffiths, J. A.; Tirrell, D. A. *J. Chem. Phys.* **1999**, *111*, 122.